

TRAIL induces necroptosis involving RIPK1/RIPK3-dependent PARP-1 activation

S Jouan-Lanhouet^{1,2}, MI Arshad^{1,2}, C Piquet-Pellorce^{1,2}, C Martin-Chouly^{1,2}, G Le Moigne-Muller^{1,2}, F Van Herreweghe³, N Takahashi³, O Sergent^{1,2}, D Lagadic-Gossmann^{1,2}, P Vandenabeele^{3,4}, M Samson^{1,2} and M-T Dimanche-Boitrel^{*,1,2}

Although TRAIL (tumor necrosis factor (TNF)-related apoptosis inducing ligand) is a well-known apoptosis inducer, we have previously demonstrated that acidic extracellular pH (pHe) switches TRAIL-induced apoptosis to regulated necrosis (or necroptosis) in human HT29 colon and HepG2 liver cancer cells. Here, we investigated the role of RIPK1 (receptor interacting protein kinase 1), RIPK3 and PARP-1 (poly (ADP-ribose) polymerase-1) in TRAIL-induced necroptosis *in vitro* and in concanavalin A (Con A)-induced murine hepatitis. Pretreatment of HT29 or HepG2 with pharmacological inhibitors of RIPK1 or PARP-1 (Nec-1 or PJ-34, respectively), or transient transfection with siRNAs against RIPK1 or RIPK3, inhibited both TRAIL-induced necroptosis and PARP-1-dependent intracellular ATP depletion demonstrating that RIPK1 and RIPK3 were involved upstream of PARP-1 activation and ATP depletion. In the mouse model of Con A-induced hepatitis, where death of mouse hepatocytes is dependent on TRAIL and NKT (Natural Killer T) cells, PARP-1 activity was positively correlated with liver injury and hepatitis was prevented both by Nec-1 or PJ-34. These data provide new insights into TRAIL-induced necroptosis with PARP-1 being active effector downstream of RIPK1/RIPK3 initiators and suggest that pharmacological inhibitors of RIPKs and PARP-1 could be new treatment options for immune-mediated hepatitis.

Cell Death and Differentiation (2012) 19, 2003–2014; doi:10.1038/cdd.2012.90; published online 20 July 2012

Tumor necrosis factor (TNF)-related apoptosis inducing ligand (TRAIL) is a key inducer of apoptosis in tumor cells¹ and a mediator of tumor immune surveillance.² TRAIL has also a crucial role in Con A-induced hepatitis.³

TRAIL activates apoptosis by binding to death receptors DR4 (TRAIL-R1) and DR5 (TRAIL-R2)⁴ in humans and only to mDR5 (mTRAIL-R2/mKILLER) in mice.⁵ Besides apoptosis induction, TRAIL induces necrosis in Jurkat cells⁶ or in murine prostate adenocarcinoma TRAMP-C2 cells.⁷ More recently, we have shown that acidic pHe switches TRAIL-induced apoptosis to RIPK1 (receptor interacting protein kinase 1)-dependent regulated necrosis in human HT29 colon adenocarcinoma and human HepG2 hepatocarcinoma cell lines.^{8,9} Such an acidic extracellular environment could occur under some pathological conditions including cancer and inflammation.^{10,11}

Necrosis has long been considered as an accidental cell death process until it has been shown that necrosis is also a well-orchestrated programmed cell death^{12,13} like apoptosis. However, there was no consensus on the specific biochemical changes, as many initiators, modulators or effectors of necrosis have been described.¹⁴ Nonetheless, some specific molecular mechanisms have been pointed out in PARP-1 (poly (ADP-ribose) polymerase-1)-mediated necrotic cell

death induced by DNA-damaging agents, called parthanatos,¹⁵ and in RIPK1-dependent programmed necrosis induced by TNF-like cytokines.¹⁶ Recently, RIPK3, another RIP family kinase, has been identified as an essential mediator for TNF-, FasL- and TRAIL-mediated necroptosis.^{17–19} This emerging necrotic pathway *in vitro* has been shown to be relevant *in vivo* in vaccinia virus infection¹⁷ and cerulein-induced pancreatitis.¹⁸

The mouse model of immune-mediated liver injury, after i.v. administration of the T-cell mitogen Con A, results in fulminant hepatitis.²⁰ Several lines of evidence suggest that NKT cells are critically involved in Con A-induced hepatitis,^{21–23} and that TRAIL expressed by these cells in the liver is directly responsible for mediating hepatic cell death.³

Here, we studied the molecular mechanisms involved in TRAIL-induced necroptosis at acidic pHe and found that TRAIL induced an early PARP-1-dependent intracellular ATP depletion, which was dependent on both RIPK1 and RIPK3 demonstrating for the first time an interrelationship between RIPK1/RIPK3 and PARP-1. We also provided evidence that Con A-induced hepatitis was a relevant model for TRAIL-induced necroptosis *in vivo*, as Nec-1 and PJ-34 protected mice from this hepatitis.

¹Université de Rennes 1, Institut de Recherche Santé Environnement et Travail (IRSET), Rennes, France; ²Institut National de la Santé et de la Recherche Médicale (INSERM), U1085, Team « Stress, Membrane and Signaling », Rennes, France; ³Molecular Signaling and Cell Death Unit, Department for Molecular Biomedical Research, VIB, Ghent, Belgium and ⁴Molecular Signaling and Cell Death Unit, Department for Biomedical Molecular Biology, Ghent University, Ghent, Belgium

*Corresponding author: M-T Dimanche-Boitrel, Team « Stress, Membrane and Signaling », IRSET/UMR INSERM 1085, Faculty of Pharmacy, 2 Av du Pr Léon Bernard, Rennes F-35043, France. Tel: + 33 223234899; Fax: + 33 223234794; E-mail: marie-therese.boitrel@univ-rennes1.fr

Keywords: TRAIL; necroptosis; colon cancer; hepatitis; concanavalin A; RIPK1/RIPK3

Abbreviations: ALT, alanine aminotransferase; AST, aspartate aminotransferase; Con A, concanavalin A; GA, geldanamycin; MEFs, mouse embryonic fibroblasts; NAC, N-acetyl-cysteine; Nec-1, necrostatin-1; NKT, natural killer T; PAR, poly ADP ribosylation; PARP-1, poly (ADP-ribose) polymerase-1; pHe, extracellular pH; RIPK1/3, receptor interacting protein kinase 1/3; ROS, reactive oxygen species; TNF, tumor necrosis factor; TRAIL, TNF-related apoptosis inducing ligand

Received 21.12.11; revised 29.5.12; accepted 13.6.12; Edited by C Borner; published online 20.7.12

Results

TRAIL-induced necroptosis at acidic pHe is dependent on RIPK1 and RIPK3. TRAIL induced apoptosis at pHe 7.4 (~25–30% of apoptotic cells) (Figure 1a, upper panel) with very low ATP depletion (Figure 1b) whereas it induced regulated necrosis at pHe 6.5 (~70% of necrotic permeabilized cells) (Figure 1a, lower panel) with high ATP depletion (~90%/NT (non-treated cells)) (Figure 1b). As TRAIL-induced necrosis was significantly inhibited by Nec-1 (Figure 1a, lower panel), a specific inhibitor of RIPK1 kinase activity, this type of cell death has been designated as necroptosis in the following text. Moreover, Nec-1 or geldanamycin (GA) pretreatment led to a switch from

necroptosis to apoptosis at acidic pHe (Figure 1a) with partial intracellular ATP repletion (Figure 1b). Then, we studied the role of RIPK1 and RIPK3 in TRAIL-induced necroptosis at acidic pHe and observed that transient transfections with siRNA targeting RIPK1 or RIPK3 almost totally reduced the expression of RIPK1 and RIPK3 in HT29 cells (Figure 1d and Supplementary Figure S1a) and significantly inhibited both TRAIL-induced necroptosis (Figure 1c, lower panel) and ATP depletion (Figure 1e). However, gene knockdown of RIPK1 and RIPK3 did not achieve complete inhibition of TRAIL-induced necroptosis at acidic pHe (Figure 1c, lower panel) probably due to increased RIPK1 and RIPK3 expression upon TRAIL treatment (data not shown). Moreover, gene knockdown of

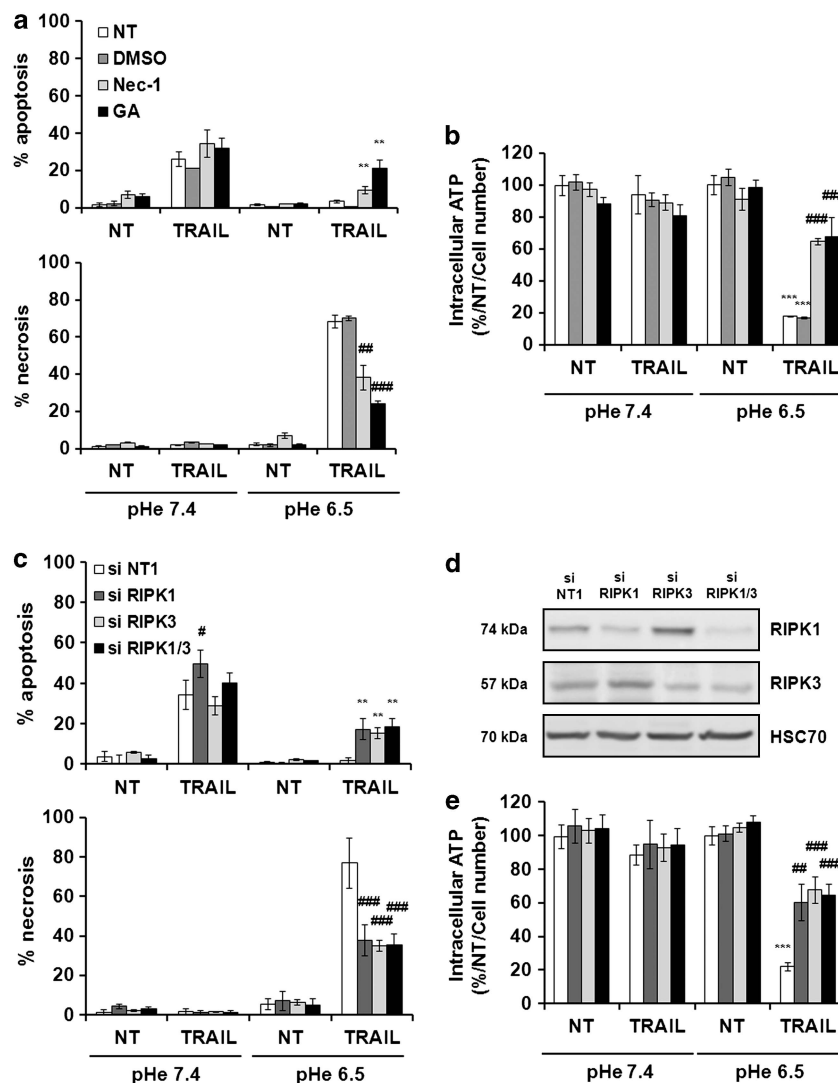


Figure 1 TRAIL-induced necroptosis at acidic pHe is dependent on both RIPK1 and RIPK3. (a) HT29 cells were treated or not (NT) with 100 ng/ml TRAIL-Flag and 2 μ g/ml anti-Flag M2 for 24 h, at physiological pHe 7.4 or acidic pHe 6.5, after a 16 h pretreatment with 1 μ M GA or a 1 h pretreatment with 100 μ M Necrostatin-1 (Nec-1). Percentages of apoptosis or necrosis were estimated as described in Materials and Methods. (b) Intracellular ATP concentration was measured as described in Materials and Methods. (c) HT29 cells were transiently transfected with the following siRNAs: si RIPK1, si RIPK3, si RIPK1/si RIPK3 (si RIPK1/3) or with si NT1 (non-targeting siRNA used as negative control). At 72 h after transfection, HT29 cells were treated with 100 ng/ml TRAIL-Flag and 2 μ g/ml anti-Flag M2 for 24 h, at pHe 7.4 or 6.5. Percentages of apoptosis or necrosis were estimated as described in Materials and Methods. (d) Western blot analysis of RIPK1 and RIPK3 expression was carried out 72 h after transfection. Anti-human HSC70 was used as a control of protein loading (one representative of three independent experiments). (e) Intracellular ATP concentration was measured as described in Materials and Methods. Mean \pm S.D. # P < 0.05, ** P < 0.01 and *** P < 0.001

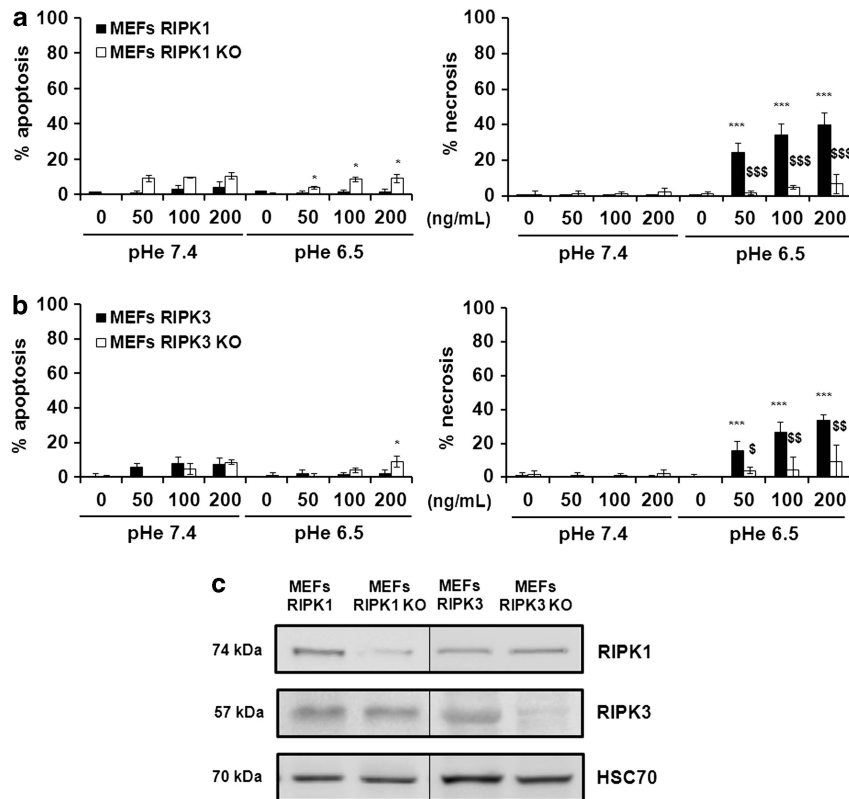


Figure 2 MEFs RIPK1 KO and MEFs RIPK3 KO are resistant to TRAIL-induced necroptosis at acidic pH. (a) MEFs RIPK1 and MEFs RIPK1 KO (b) MEFs RIPK3 and MEFs RIPK3 KO were treated with the indicated TRAIL-Flag concentrations cross-linked with 2 μ g/ml anti-Flag M2 for 24 h, at pH 7.4 or 6.5. Percentages of apoptosis and necrosis were estimated as described in Materials and Methods. (c) Western blot analysis of RIPK1 and RIPK3 expression was performed. Anti-human HSC70 was used as a control of protein loading (one representative of three independent experiments). Mean \pm S.D. * $P < 0.05$, ** $P < 0.01$ and *** $P < 0.001$

RIPK1 and/or RIPK3 led to a switch from TRAIL-induced necroptosis to apoptosis at acidic pH with partial restoration of intracellular ATP level (Figures 1c and e). We then tested mouse embryonic fibroblasts (MEFs) from *Ripk1*^{-/-} and *Ripk3*^{-/-} mice with respective littermate WT controls. Both WT MEFs (MEFs RIPK1 and MEFs RIPK3) were resistant to TRAIL-induced apoptosis at physiological pH (Figures 2a and b, left panels) but were sensitized to TRAIL-induced necroptosis at acidic pH (Figures 2a and b, right panels). As expected, TRAIL-induced necroptosis at acidic pH was almost completely inhibited in MEFs RIPK1 KO and MEFs RIPK3 KO, which do not express RIPK1 or RIPK3, respectively, (Figure 2c and Supplementary Figure S1b), confirming a role for both RIPK1 and RIPK3 in TRAIL-induced necroptosis at acidic pH.

Interestingly, an acidic pH sensitized HT29 cells only to TRAIL-induced cell death but not to FasL or TNF (Supplementary Figure S2a, right panel), although the pro-death activities of FasL or TNF in Jurkat or L929 cells were not impaired, respectively (data not shown). TRAIL-induced cell death in HT29 cells was inhibited by the use of antagonistic antibodies directed against DR4 or DR5, but not by an antagonistic antibody directed against Fas or by a TNF inhibitor (Supplementary Figure S2b). However, anti-Fas or TNF inhibitor inhibited FasL-induced cell death in Jurkat cells or TNF-induced cell death in L929 cells, respectively

(Supplementary Figures S2c and d). Moreover, transient transfection of HT29 cells with siRNA targeting DR4, DR5, Fas or TNF-R1 led to a decreased expression of DR4, DR5, Fas or TNF-R1, respectively (Supplementary Figures S3b and c), but only reduced expression of DR4 and DR5 inhibited TRAIL-induced necroptosis at acidic pH (Supplementary Figure S3a, right panel). Besides, transient transfection of Jurkat with siRNA targeting Fas or L929 cells with siRNA targeting TNF-R1, significantly inhibited FasL-induced cell death and TNF-induced cell death, respectively (Supplementary Figures S4a–d). Finally, upon TRAIL treatment at physiological or acidic pH, very low concentrations of TNF were secreted by HT29 cells (Supplementary Figure S4e). All these data suggested that TRAIL-induced necroptosis at acidic pH was only triggered via TRAIL death receptors (DR4 or DR5) independently of TNF secretion.

RIPK1/RIPK3-dependent PARP-1 activation initiates TRAIL-induced necroptosis at acidic pH. PARP-1 activity was not detected in HT29 cells treated with TRAIL at pH 7.4 but was increased between 4 and 16 h after TRAIL treatment at acidic pH (Figure 3a, upper panel). Protein poly ADP-ribosylation (PAR), analyzed by western blot, increased accordingly (Figure 3a, lower panel and Supplementary Figure S5a). To confirm the role of PARP-1, transient transfection with siRNA targeting PARP-1 almost totally

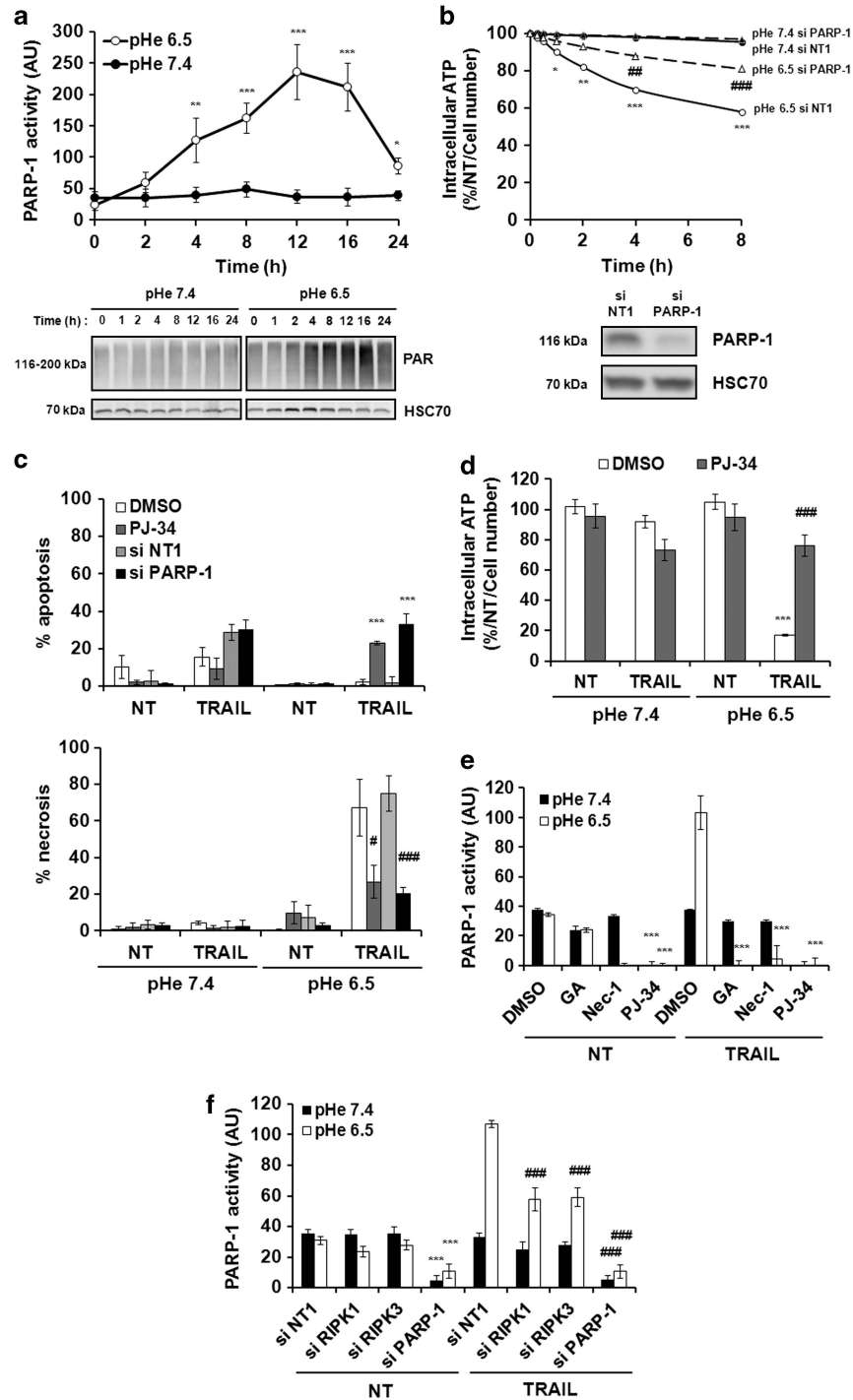


Figure 3 RIPK1/RIPK3-dependent PARP-1 activation initiates TRAIL-induced necroptosis at acidic pH. (a) HT29 cells were treated with 100 ng/ml TRAIL-Flag and 2 μ g/ml anti-Flag M2 for the indicated times, at pH 7.4 or 6.5. PARP-1 activity was determined as described in Materials and Methods. Western blot analysis of protein poly ADP-ribosylation (PAR) was carried out. Anti-human HSC70 was used as a control of protein loading (one representative of three independent experiments). (b) HT29 cells were transiently transfected with a siRNA directed against PARP-1 or with si NT1 (non-targeting siRNA used as negative control). At 72 h after transfection, cells were treated as above. Intracellular ATP concentration was measured as described in Materials and Methods. Western blot analysis of PARP-1 expression was carried out 72 h after transfection. Anti-human HSC70 was used as a control of protein loading (one representative of three independent experiments). (c) HT29 cells were transiently transfected with si NT1 or si PARP-1 for 72 h, or were pretreated for 1 h with DMSO or 10 μ M PJ-34. Then, HT29 cells were treated or not (NT) with 100 ng/ml TRAIL-Flag and 2 μ g/ml anti-Flag M2 for 24 h, at pH 7.4 or 6.5. Percentages of apoptosis and necrosis were estimated as described in Materials and Methods. (d) Intracellular ATP concentration was measured as described in Materials and Methods. (e) HT29 cells were treated or not (NT) with 100 ng/ml TRAIL-Flag and 2 μ g/ml anti-Flag M2 for 4 h, at pH 7.4 or 6.5, after a pretreatment or not (DMSO) with 1 μ M GA for 16 h, 100 μ M Nec-1 or 10 μ M PJ-34 for 1 h. PARP-1 activity was determined as described in Materials and Methods. (f) HT29 cells were transiently transfected with the following siRNAs: si RIPK1, si RIPK3, si PARP-1 or with si NT1 for 72 h, and then treated with TRAIL as above. PARP-1 activity was determined as described in Materials and Methods. Mean \pm S.D. *, # P <0.05, **, ## P <0.01 and ***, ### P <0.001

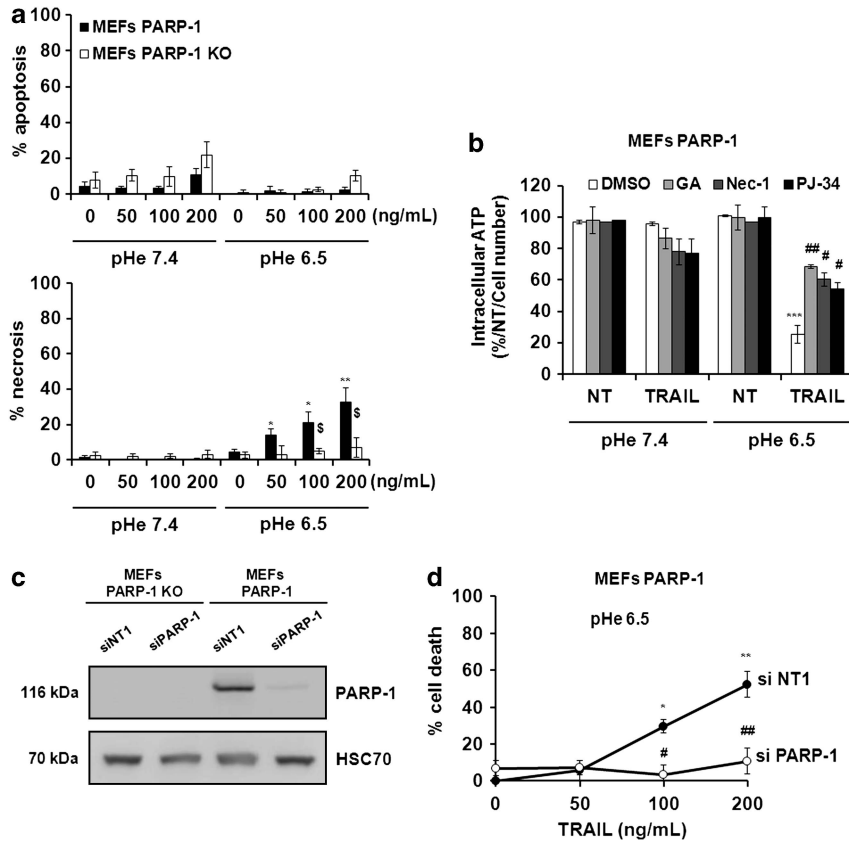


Figure 4 Additional evidence for the role of PARP-1 in TRAIL-induced necroptosis at acidic pHe. (a) MEF PARP-1 and MEF PARP-1 KO cells were treated with the indicated TRAIL-Flag concentrations cross-linked with 2 μ g/ml anti-Flag M2 for 24 h, at pHe 7.4 or 6.5. Percentages of apoptosis and necrosis were estimated as described in Materials and Methods. (b) MEF PARP-1 cells were treated with 100 ng/ml TRAIL-Flag and 2 μ g/ml anti-Flag M2 for 24 h, at pHe 7.4 or 6.5, after a pretreatment or not (DMSO) with 1 μ M GA for 16 h, 100 μ M Nec-1 or 10 μ M PJ-34 for 1 h. Intracellular ATP concentration was measured as described in Materials and Methods. (c) MEF PARP-1 KO and MEF PARP-1 cells were transiently transfected for 72 h with si NT1 (non-targeting siRNA used as negative control) or si PARP-1. Western blot analysis of PARP-1 expression was performed. Anti-human HSC70 was used as a control of protein loading (one representative of three independent experiments). (d) MEF PARP-1 cells were transiently transfected with si NT1 or si PARP-1 for 72 h, and then treated with the indicated TRAIL-Flag concentrations cross-linked with 2 μ g/ml anti-Flag M2 for 24 h, at pHe 7.4 or 6.5. Percentage of cell death was estimated by a methylene blue viability assay as described in Materials and Methods. Mean \pm S.D. *, #, \$ P < 0.05, **, ## P < 0.01 and *** P < 0.001

reduced PARP-1 expression in HT29 cells (inset Figure 3b and Supplementary Figure S5b), inhibited TRAIL-induced ATP depletion (Figure 3b) and necroptosis at acidic pHe (Figure 3c, lower panel) and switched to TRAIL-induced apoptosis (Figure 3c, upper panel). Moreover, pretreatment with PJ-34, a pharmacological inhibitor of PARP-1, switched from TRAIL-induced necroptosis to apoptosis and partially restored intracellular ATP levels (Figures 3c and d). Pretreatment with PJ-34 or gene knockdown of PARP-1 by RNA interference completely inhibited TRAIL-induced PARP-1 activation at acidic pHe (Figures 3e and f). Moreover, pretreatment with GA or Nec-1, or gene knockdown of RIPK1 or RIPK3 by RNA interference inhibited TRAIL-induced PARP-1 activation at acidic pHe (Figures 3e and f), suggesting that RIPK1/RIPK3-dependent signaling is required for PARP-1 activation. In accordance with the above results obtained with HT29 cells, MEFs PARP-1 KO cells were more resistant than WT MEFs (MEFs PARP-1) to TRAIL-induced necroptosis at acidic pHe (Figure 4a, lower panel). Moreover, TRAIL-induced ATP depletion at acidic pHe was partially inhibited by pretreatment of MEFs PARP-1

with GA, Nec-1 or PJ-34 (Figure 4b), suggesting a role for RIPK1 and PARP-1 in TRAIL-induced necroptosis at acidic pHe. Transient transfection of MEFs PARP-1 with siRNA targeting PARP-1 decreased PARP-1 expression (Figure 4c and Supplementary Figure S5c) and rendered these cells more resistant to TRAIL-induced cell death at acidic pHe (Figure 4d). Finally, gene knockdown of RIPK1, RIPK3 or PARP-1 by RNA interference in human HepG2 hepatocarcinoma cells inhibited TRAIL-induced necroptosis at acidic pHe and led to a switch from necroptosis to apoptosis with restoration of intracellular ATP level (Figures 5a and b). All these data confirmed a role for PARP-1, RIPK1 and RIPK3 in TRAIL-induced necroptosis at acidic pHe in HT29, MEFs and HepG2 cells.

ROS production is not involved in TRAIL-induced necroptosis at acidic pHe. As reactive oxygen species (ROS) generation has been involved in TNF-induced necrosis^{24,25} and as ROS-mediated DNA damage might contribute to activation of PARP-1, we looked for such a role. We first measured ROS generation by flow cytometry using

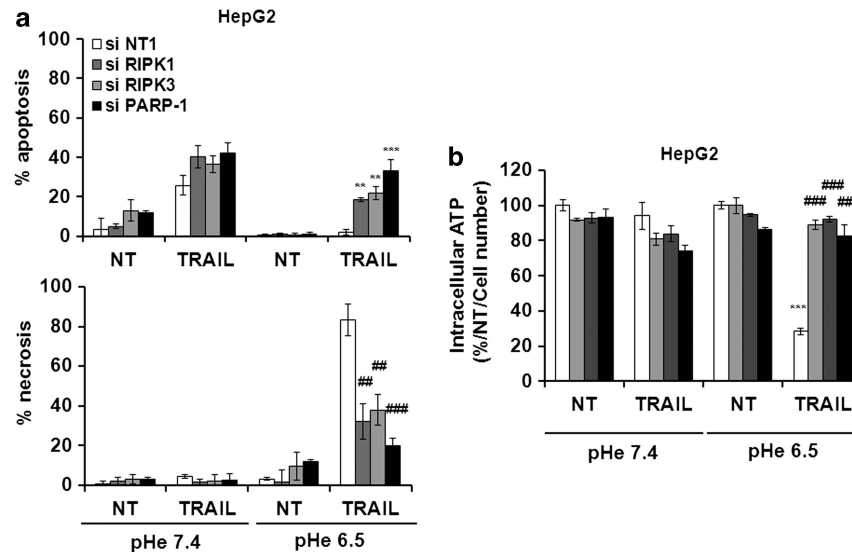


Figure 5 Role of PARP-1, RIPK1 and RIPK3 in TRAIL-induced necroptosis at acidic pH, in HepG2 cells. (a) HepG2 cells were transiently transfected for 72 h with si NT1 (non-targeting siRNA used as negative control) or with siRNAs directed against RIPK1, RIPK3 or PARP-1, and then treated with 100 ng/ml TRAIL-Flag and 2 μ g/ml anti-Flag M2 for 24 h, at pHe 7.4 or 6.5. Percentages of apoptosis and necrosis were estimated as described in Materials and Methods. (b) Intracellular ATP concentration was measured as described in Materials and Methods. Mean \pm S.D. **, ## $P < 0.01$ and ***, ### $P < 0.001$

dihydroethidium probe. We observed an important ROS production (superoxide anion, $O_2^{\cdot-}$) in HT29 cells, from 12 to 24 h after TRAIL treatment at acidic pHe (Supplementary Figure S6a). ROS generation 24 h after TRAIL treatment at acidic pHe or after menadione treatment was inhibited by several antioxidants (Thiourea, *N*-acetyl-cysteine (NAC) and TEMPOL) (Supplementary Figures S6b and c). However, TRAIL-induced necroptosis (Supplementary Figure S7a), PARP-1 activation (Supplementary Figure S7b) or intracellular ATP depletion (Supplementary Figure S7c) at pHe 6.5 were not inhibited by NAC or TEMPOL, which were able to inhibit ROS-dependent cell death induced by propionate/acetate in HT29 cells²⁶ (Supplementary Figures S7d and e). Altogether, these results suggested that TRAIL-induced necroptosis at acidic pHe involved a RIPK1/RIPK3-dependent PARP-1 activation pathway independent of ROS production leading to high ATP depletion.

Con A-induced hepatitis is inhibited by Nec-1 or PJ-34 pretreatment. As CD1d-deficient (CD1d KO) mice have been shown to be protected from Con A-induced hepatitis demonstrating a role for NKT cells^{21–23} and TRAIL has been shown to have a crucial role in Con A-induced hepatitis,³ we questioned whether TRAIL-induced necroptosis has a causal role in this model. Pathological examination of liver tissues stained with Hematoxylin/Eosin showed that a single injection of Con A led to a clear liver damage as presented by large diffused perivascular and parenchymal zones of necrosis observed at 6 h or 10 h in WT (data not shown) but not in CD1d KO mice, confirming a role for NKT cells in Con A-induced hepatitis. These histological findings were corroborated with biochemical findings showing that levels of aspartate aminotransferase (AST) and alanine aminotransferase (ALT) were elevated in serum of WT mice but were very low in serum of CD1d KO mice at 6 and 10 h after Con A

injection (Figure 6a). As TRAIL has been shown to have a crucial role in Con A-induced hepatitis, we performed RT-qPCR to determine mRNA levels of TRAIL and its death receptor DR5 in mouse liver tissues. TRAIL and DR5 mRNA levels were increased at 6 and/or 10 h after Con A injection in WT but not in CD1d KO mice (Figure 6b, left and right panels, respectively).

Besides, the mode of hepatic cell death induced by Con A was rather necrotic than apoptotic, as a time-dependent decrease of intracellular LDH level and very low caspase-3 activity were measured in lysates of liver tissues from Con A-treated WT mice (Figures 6c and d). We also observed an increased expression of necrotic markers such as HMGB1 and cyclophilin A in lysates of liver tissues from Con A-treated mice at 6 and 10 h after ConA injection (Figure 6e and Supplementary Figure S8a). Interestingly, intracellular LDH levels were preserved in lysates of liver tissues from Con A-treated CD1d KO mice confirming protection of these mice against Con A-induced hepatitis (Figure 6c).

Next, we looked for a role of PARP-1. PARP-1 activity was increased at 6 and 10 h after Con A injection in lysates of liver tissues from WT mice but not in those from CD1d KO mice (Figure 7a). Accordingly, PAR residues formation, analyzed by western blot in lysates of liver tissues, was increased at 6 and 10 h after Con A injection in WT but not in CD1d KO mice (Figure 7b). The Spearman Rank Correlation analyses to compare ALT or AST serum levels with PARP-1 activity after Con A injection in WT mice demonstrated a positive correlation between these biological markers of hepatic injury (Spearman $r = 0.8166$, $P < 0.001$ for AST/PARP-1 and Spearman $r = 0.7669$, $P < 0.05$ for ALT/PARP-1) (Figure 7c).

At last, to investigate the role of RIPK1 and PARP-1 in Con A-induced hepatitis, WT mice were pretreated with Nec-1, PJ-34 or both inhibitors before Con A injection. Pretreatment with either Nec-1 or PJ-34 significantly decreased Con A-induced

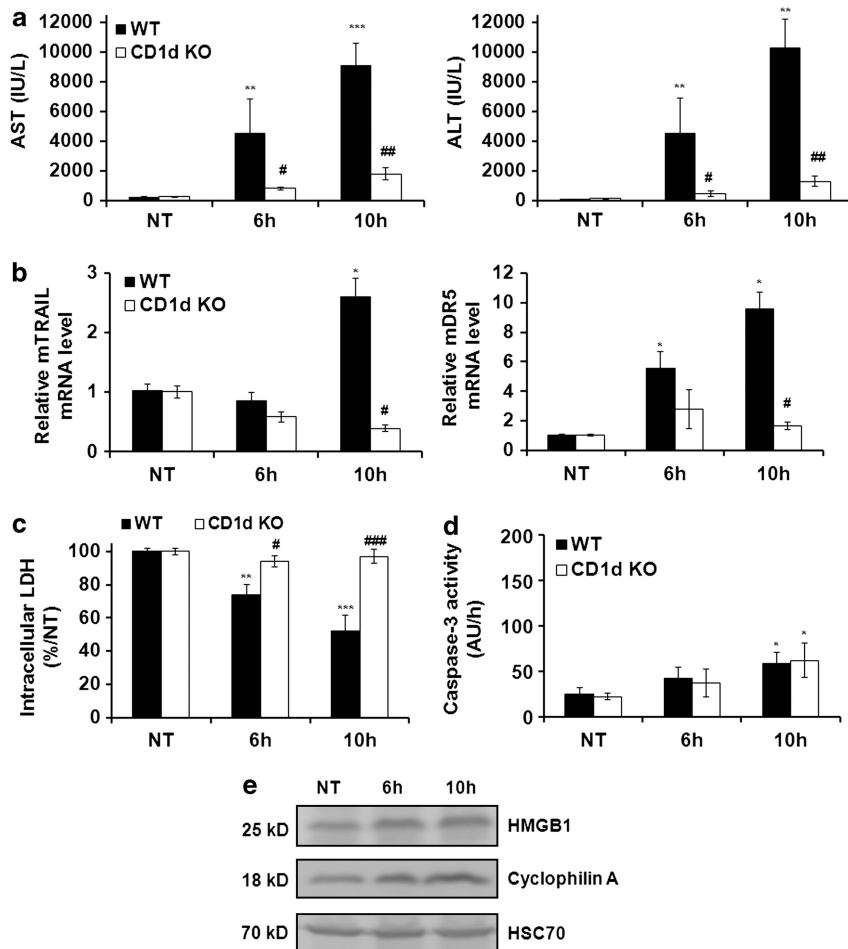


Figure 6 Con A-induced hepatitis requires NKT cells and is associated with TRAIL-induced necrotic cell death. WT and CD1d KO C57Bl/6 mice were treated with 20 mg/kg Con A for 6 h (WT, $n=6$; CD1d KO, $n=7$) or 10 h (WT, $n=7$; CD1d KO, $n=6$). Control mice were treated with PBS only (NT, WT, $n=7$; CD1d KO, $n=6$). (a) Serum levels of ALT and AST were determined as described in Materials and Methods. (b) Relative mTRAIL and mDR5 mRNA levels were determined by RT-qPCR in liver tissues as described in Materials and Methods. (c) Intracellular LDH levels were measured in lysates of liver tissues as described in Materials and Methods. (d) Caspase-3 activity was measured in lysates of liver tissues as described in Materials and Methods. (e) Western blot analysis of HMGB1 or cyclophilin A was carried out in lysates of liver tissues. Anti-human HSC70 was used as a control of protein loading (one representative of three experiments). Mean \pm S.D. * $P < 0.05$, ** $P < 0.01$ and *** $P < 0.001$

hepatotoxicity (Figure 8a, see arrows), associated AST/ALT serum levels (Figure 8b) and PARP activation in lysates from affected liver tissue (Figure 8c). This suggests a potential role of RIPK1 and PARP-1 in this type of hepatic injury. Interestingly, Con A-induced PARP-1 activation (Figure 8c) and increased PAR residues formation (Figure 8d and Supplementary Figure S8b) were significantly attenuated in lysates of liver tissues from mice pretreated with Nec-1, suggesting that RIPK1 might be involved upstream of PARP-1 activity. In agreement with a hepatic necrotic death, no proteolytic fragments of caspase-3 (p32 \rightarrow p17 and p10) and PARP-1 (p116 \rightarrow p84) were detected in lysates of liver tissues from mice treated with Con A (Figure 8d and Supplementary Figure S8b). Moreover, the increase in PARP-1 expression in liver tissues after Con A treatment (Supplementary Figure S8b) was inhibited by pretreatment with Nec-1 or PJ-34 (Figure 8d). All these data pointed out that Con A-induced hepatitis is mediated by TRAIL-induced necroptosis driven by RIPK1. We did not observe any increased protective effect when both inhibitors were combined (Figures 8b and c).

Moreover, Con A-induced increase in PARP-1 expression and protein poly ADP-ribosylation were inhibited to the same extent by either Nec-1 or PJ-34 or the combination (Figure 8d). Altogether, these data suggest that PARP-1 activation has a significant role in Con A-induced hepatitis and that RIPK1 and PARP-1 constitute a major cell death signaling pathway.

Discussion

We reported earlier that TRAIL induces a RIPK1-dependent necrosis-like cell death pathway at acidic pH.⁹ We further investigated here the underlying molecular mechanisms involved in this cell death pathway. By using Nec-1, an RIPK1 allosteric inhibitor,²⁷ and RNA interference targeting RIPK1 or RIPK3, we demonstrated that TRAIL-induced cell death at acidic pH can indeed be defined as necroptosis and depends on both RIPK1 and RIPK3. The role of RIPK1 and RIPK3 was clearly confirmed in MEFs derived from *ripk1* and *ripk3* knockout mice, as in both MEFs TRAIL-induced necroptosis

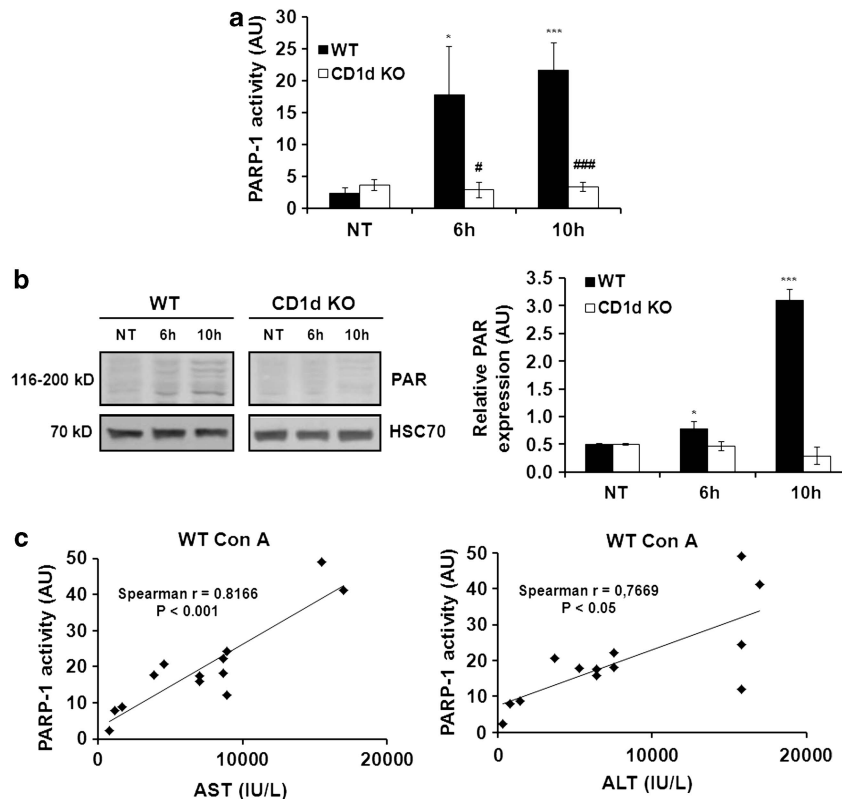


Figure 7 PARP-1 is activated in Con A-induced hepatitis. WT and CD1d KO C57Bl/6 mice were treated as in Figure 6. (a) PARP-1 activity was determined as described in Materials and Methods. (b) Western blot analysis of PAR expression was carried out in lysates of liver tissues. Anti-human HSC70 was used as a control of protein loading (one representative of three experiments). Densitometry analysis of PAR expression was carried out (three independent western blot experiments). Relative PAR expression was expressed in arbitrary units (AU) as percentage of absorbance measured in NT. (c) Graphic representation of the Spearman's rank correlation analysis between AST/ALT and PARP-1 activity. Mean \pm S.D. *, # P < 0.05 and ***, ### P < 0.001

at acidic pH was completely inhibited in contrast to control MEFs. Moreover, an acidic pH sensitized HT29 cells only to TRAIL-induced cell death but not to TNF or FasL. And only decreased expression of DR4 or DR5 by RNA interference, or use of antagonistic antibodies directed against DR4 and DR5, significantly inhibited TRAIL-induced necroptosis showing that TRAIL-induced necroptosis at acidic pH was specific of the TRAIL death pathway. Although a TNF autocrine production is implicated in zVAD-fmk-induced necroptosis in L929 cells,²⁸ it was not involved in TRAIL-induced necroptosis at acidic pH, as we observed no inhibition of this cell death pathway by using a TNF inhibitor and low increased production of TNF by ELISA.

Although the effector mechanisms of apoptosis are well defined, little is known about those involved in regulated necrosis.²⁹ The role of mitochondrial ROS in necrosis has been previously shown.²⁴ And recent data have demonstrated that RIPK1 and RIPK3 act upstream mitochondria to regulate ROS production during regulated necrosis.^{17,19} However, ROS are not required for regulated necrosis in all cell types, particularly in U937, HT29 or Jurkat cells.^{18,30} Accordingly, we demonstrated here that TRAIL-induced necroptosis at acidic pH was not inhibited in HT29 cells by Thiourea, NAC or TEMPOL, three antioxidants. However, we found a clear link between RIPK1/RIPK3 and PARP-1 activation in TRAIL-induced necroptosis at acidic pH. PARP-1 has been critically

implicated in the necroptosis induced by TNF in L929 cells³¹ and more recently in parthanatos.^{15,32} Our data showed that PARP-1 activity increased with time during the course of TRAIL-induced necroptosis and concomitantly resulted in increased ATP depletion. Indeed, PJ-34, a pharmacological inhibitor of PARP-1, and RNA interference targeting PARP-1 inhibited TRAIL-induced ATP depletion leading to a switch from necroptosis to apoptosis at acidic pH, thus further supporting an active role of PARP-1 in determining the mode of death receptor-induced cell death.³¹ Such a switch was also observed after Nec-1 or GA pretreatment (Meurette *et al.*⁹ and present data). Our previous and present data are in agreement with literature reporting that GA induced a switch from TNF-induced necroptosis to apoptosis.³³ Moreover, the role of PARP-1 in TRAIL-induced necroptosis at acidic pH was confirmed in *parp-1* KO MEFs, in which cell death was completely inhibited. In addition, knockdown of PARP-1 mRNA in MEFs rendered these cells more resistant to TRAIL-induced cell death. Interestingly, Nec-1 and knockdown of RIPK1 or RIPK3 revealed that TRAIL-induced PARP-1 activation at acidic pH was dependent on both RIPK1 and RIPK3, suggesting that these two kinases most likely act upstream of PARP-1 and ATP depletion during necroptosis. Until now, RIPK1 activation leading to mitochondrial dysfunction has been shown to occur downstream of PARP-1 activation in DNA alkylating agent-induced necrosis,³⁴

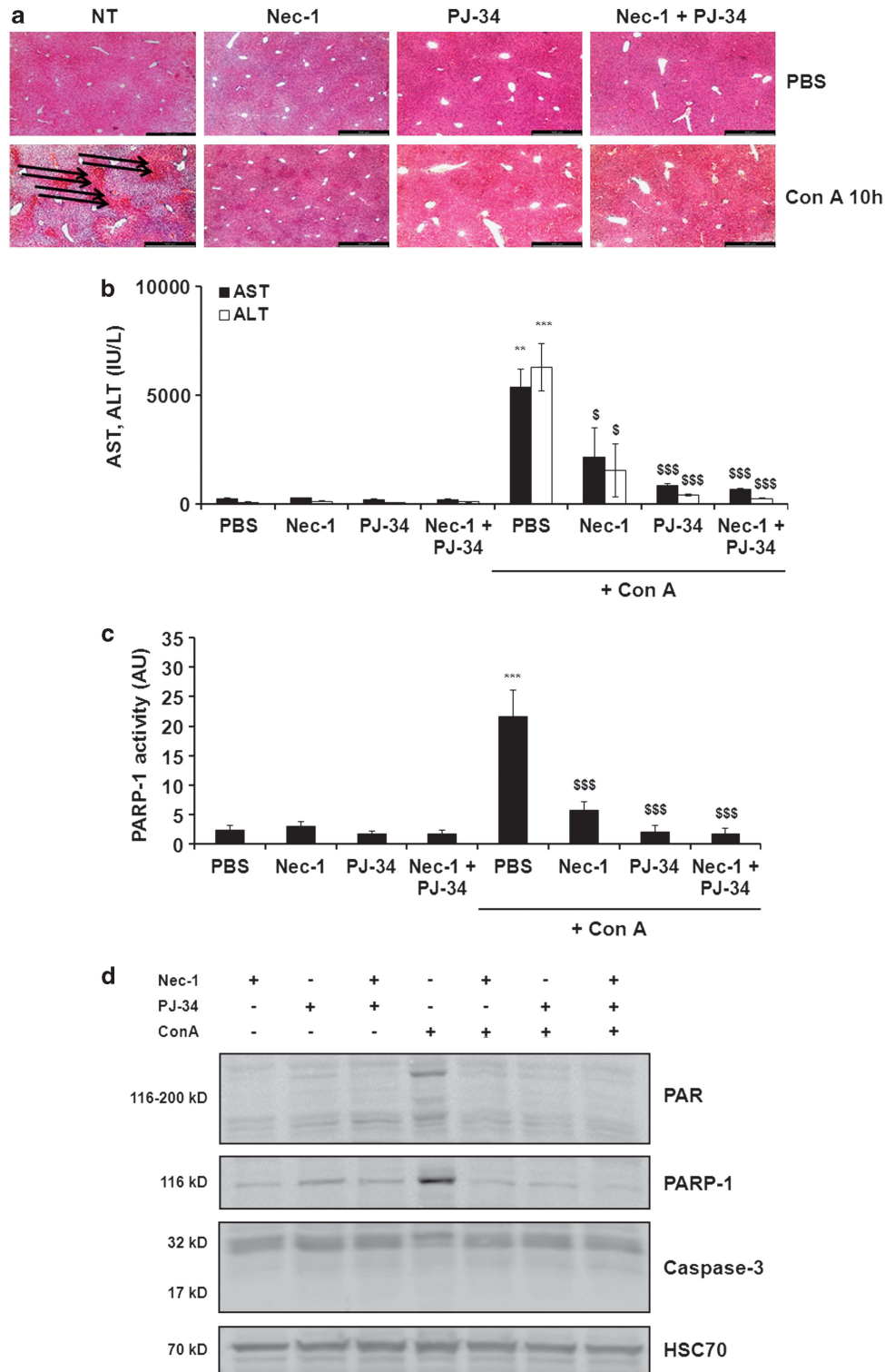


Figure 8 RIPK1 kinase and PARP-1 are involved in Con A-induced hepatitis. C57Bl/6 WT mice were pretreated or not (NT) with 10 mg/kg PJ-34 for 1 h, 125 μ g Nec-1 for 15 min, or with both inhibitors before treatment or not with 12 mg/kg Con A for 10 h (PBS, $n=7$; PBS + Con A, $n=10$; Nec-1 + Con A, $n=6$; PJ-34 + Con A, $n=6$; PJ-34 + Nec-1 + Con A, $n=7$; Nec-1 + PBS, $n=7$; PJ-34 + PBS, $n=7$; PJ-34 + Nec-1 + PBS, $n=7$). (a) Hematoxylin- and Eosin-stained liver sections were shown. Scale bars represent 200 μ m. (b) ALT and AST serum levels were determined as described in Materials and Methods. (c) PARP-1 activity was determined in lysates of liver tissues as described in Materials and Methods. (d) Western blot analysis of protein poly ADP-ribosylation (PAR), PARP-1 and caspase-3 expression was carried out. Anti-human HSC70 was used as a control of protein loading (one representative of three experiments). Mean \pm S.D. $^{\$}P<0.05$, $^{**}P<0.01$ and $^{***, $$$}P<0.001$

and the relationship between this cell death process and necroptosis remains unclear. More studies are needed to understand the relationship between RIPK1/RIPK3 and PARP-1 activation in TRAIL-induced necroptosis at acidic pH. It has been suggested that PARP-1 activity may be regulated by phosphorylation.³⁵ Therefore, it is tempting to speculate that PARP-1 might be a direct or indirect substrate for RIPK1- and/or RIPK3-mediated kinase cascade.

Besides, NKT cells and TRAIL have been shown to have a crucial role in Con A-induced hepatitis and liver damage (large area of necrosis) was associated with high serum levels of AST and ALT.^{3,22} Accordingly, we reported increased TRAIL mRNA expression levels in the liver of Con A-treated WT mice but not in Con A-treated CD1d KO mice suggesting that the increase might be confined to certain immune cells such as NKT cells. In line with this, we observed increased mDR5 mRNA levels in liver of Con A-treated animals, which could mediate hepatocyte cell death induced by TRAIL-expressing NKT cells. Increased expression of HMGB1 and cyclophilin A in the liver of Con A-treated mice are other evidence in favor of ongoing necrosis.^{36,37} Moreover, we demonstrated that Con A injection activated PARP-1 in the liver of WT mice but not of CD1d KO mice. In agreement with our *in vitro* data showing high PARP-1 activation during TRAIL-induced necroptosis at acidic pH, high PARP-1 activity was correlated with liver damage and high AST/ALT serum levels in WT mice treated with Con A. Moreover, we observed an increased PARP-1 expression in injured liver tissues suggesting that PARP-1 may serve as a biological marker of Con A-induced hepatitis. Interestingly, pretreatment of mice with Nec-1 significantly protected mice from Con A-induced hepatitis by decreasing serum AST/ALT levels, PARP-1 expression and PARP-1 activation in the liver suggesting a role for RIPK1 upstream of PARP-1 in necrosis of hepatocytes. This was confirmed by the protective effect of Nec-1 and PJ-34 on Con A-induced hepatitis. However, no increased protective effect was shown when combining both inhibitors.

All these data suggest that Con A-induced hepatitis may be a relevant *in vivo* model of TRAIL-induced necroptosis at acidic pH, as it involves the TRAIL/mDR5 pathway and the RIPK1/PARP-1 axis. The role of RIPK3 in Con A-induced hepatitis remains to be determined. The required acidic conditions during Con A-induced hepatitis or TRAIL-mediated necroptosis could be generated by the inflamed liver environment,³⁸ which could lead to acidification of the extracellular environment.¹⁰

Necrotic death is associated with diverse pathological conditions, including myocardial infarction, cerebral ischemia, acute organ failure and infection.¹⁶ The *in vitro* and *in vivo* models of TRAIL-induced necroptosis described in this work may be the basis to identify new modulators or inhibitors. These drugs would be particularly useful in the treatment of degenerative diseases where necrotic pathways are involved. In addition, programmed necrosis could be triggered to induce cell death in apoptotic/drug-resistant cancers against chemotherapy to counteract the 'Achilles heel' of cancers.³⁹ In this context, in solid tumors with acidic pH, TRAIL may be an efficient inducer of necroptosis and the release of damage-associated molecular pattern molecules and proinflammatory cytokines may favor the recruitment of immune cells leading

to tumor regression. In conclusion, our findings provide evidence that TRAIL-induced necroptosis involves RIPK1/RIPK3-dependent PARP-1 activation.

Materials and Methods

Chemicals and antibodies. Recombinant human Flag-tagged TRAIL and Flag-tagged FasL, recombinant human TNF- α , Necrostatin-1 (Nec-1) and PJ-34 were obtained from Alexis Biochemicals (Enzo Life Sciences, Villeurbanne, France). Propidium iodide, Methylene blue, NAC, TEMPOL, Menadione, acetate and propionate sodium salts, concanavalin A (Con A) and anti-Flag M2 IgG1 antibody were obtained from Sigma-Aldrich (Lyon, France). Hoechst 33342 was obtained from Invitrogen (Life Technologies, Villebon sur Yvette, France). GA and pan-caspase inhibitor (z-VAD) were obtained from Calbiochem (VWR International, Fontenay-sous-Bois, France). Thiourea was obtained from Fluka (Sigma-Aldrich). Bradford reagent was obtained from Bio-Rad (Marnes-la-Coquette, France). Proteases inhibitors cocktail and PHOSstop were obtained from Roche (Roche Applied Science, Meylan, France).

Antagonistic mouse monoclonal antibodies directed against extracellular domain of human TRAIL-R1/DR4 and TRAIL-R2/DR5 were from Alexis Biochemicals. The antagonistic mouse monoclonal antibody directed against Fas receptor (ZB4) was from Immunotech (Beckman Coulter, Marseille, France). The TNF α inhibitor (Etanercept, TNFR2 (p75)-IgG1) was obtained from Amgen (Thousand Oaks, CA, USA).

Antibodies used for immunoblotting were mouse monoclonal antibodies to RIPK1 (clone 38), PARP-1 (clone 7D3-6) (Becton Dickinson, Le Pont de Claix, France), PAR (clone 10H) (Alexis Biochemicals), TNFR1 (clone H-5) and HSC70 (clone B-6) (Santa-Cruz, Tebu, Le Perray en Yvelines, France); rabbit polyclonal antibodies to TRAIL-R1/DR4, TRAIL-R2/DR5 (ProSci Incorporated, Interchim, Montluçon, France), PAR (Alexis Biochemicals), Fas/CD95 (clone C-20), Caspase-3 (clone H-277) (Santa-Cruz), HMGB1 (Sigma-Aldrich), Cyclophilin A, PARP-1 (clone 46D11) and RIPK1 (Cell Signaling Technology, St. Quentin, France) and goat polyclonal antibodies to RIPK3 (clone N-14) (Santa-Cruz). Horseradish-peroxidase-conjugated secondary antibodies were provided by Dako France (Trappes, France) and Upstate Technology Incorporated (Milton Keynes, UK).

Cell culture. Human HT29 colon carcinoma, HepG2 hepatocarcinoma and Jurkat lymphoma cell lines were obtained from ATCC (American Type Culture Collection, Rockville, MD, USA) and cultured in EMEM (Eurobio, les Ulis, France), DMEM high glucose (Invitrogen) or RPMI (Invitrogen), respectively, supplemented with 10% FBS (Invitrogen) and 2 mM L-glutamine (Invitrogen). Mouse L929 cell line was a gift from Vandebeele lab (VIB, Ghent University, Belgium) and cultured in DMEM high glucose supplemented with 10% FCS and 2 mM L-glutamine. Immortalized A1.47 MEFs (MEFs PARP-1 KO) and C9 MEFs (MEFs PARP-1) were a gift of Girish Shah (University of Laval, Canada) and cultured as previously described.⁴⁰ Immortalized MEFs RIPK1 and MEFs RIPK1 KO (prepared by Linde Duprez, Vandebeele lab, VIB, Ghent University, Belgium), primary MEFs RIPK3 and MEFs RIPK3 KO (prepared by Mathieu Bertrand, Vandebeele lab, VIB, Ghent University, Belgium) were cultured in DMEM high glucose supplemented with 10% FCS and 2 mM L-glutamine. All cells were cultured under a 5% CO₂ atmosphere at 37°C.

Cell treatments. To set the pH of culture medium to either 7.4 or 6.5, we supplemented medium without sodium hydrogenocarbonate (Eurobio) with 23 mM or 5 mM sodium hydrogenocarbonate, respectively, in an atmosphere of 5% CO₂. For all experiments, cells were treated in proliferative conditions.

Cell death assays. Cell viability was assessed by a methylene blue colorimetric assay. Briefly, cells were seeded in MW96 at a density of 30 000 cells/well. After treatment, cells were washed in PBS and fixed for 30 min in 95% ethanol. Following removal of ethanol, fixed cells were dried and colored for 40 min in methylene blue. After two washes in tap water, 100 μ l of 0.1 N HCl per well were added. Plates were then analyzed with a spectrometer at 620 nm (VersaMax Microplate Reader, Molecular Devices, Wokingham Berkshire, UK) with SoftMax Pro Software. The percentage of viability was calculated by the following formula: $100 \times (\text{optical density values of treated cells} / \text{optical density values of non-treated cells})$.

Microscopic detection of apoptosis or necrosis was carried out in both floating and adherent cells recovered after TRAIL treatment using nuclear chromatin staining with 1 μ g/ml Hoechst 33342 and 1 μ g/ml propidium iodide for 15 min at

37°C. Apoptotic cells (i.e., with condensed blue chromatin or fragmented blue nuclei) or necrotic cells (i.e., with non-fragmented red nuclei) were counted in comparison with total population ($n=300$ cells).

Caspase-3 activity assay. Caspase-3 activity was measured by monitoring fluorescence continuously in a dual luminescence fluorimeter (Spectra max Gemini XS, Molecular Devices). Briefly, 50–80 μ g of cell lysates obtained in a lysis buffer (50 mM HEPES pH 7.5, 150 mM NaCl, 1 mM EGTA pH 7.4, 0.1% Tween, 10% glycerol, 1 mM DTT) were incubated at 37°C in a caspase assay buffer (20 mM PIPES pH 7.2, 100 mM NaCl, 10% sucrose, 1 mM EDTA, 0.1% CHAPS, 1 mM dithiothreitol) containing 80 μ M of DEVD-AMC (Sigma-Aldrich). Enzyme activities were determined as initial velocities and expressed as relative intensity/hour.

LDH concentration measurement. LDH concentration was measured with the CytoTox-One homogenous membrane integrity assay (Promega, Charbonnières, France) according to the manufacturer's instructions. LDH concentration was expressed as %/NT.

ATP concentration measurement. ATP concentration was measured using the CellTiter-Glo Luminescent Cell Viability Assay kit (Promega). Briefly, cells were seeded in MW96 at a density of 30 000 cells/well. Half an hour before the end of treatment, cells were allowed to equilibrate to room temperature. Then, medium was thrown, cells were lysed in the provided buffer and the luminescent substrate was added. Luminescence was measured in a dual luminescence fluorimeter (Spectra max Gemini XS). In parallel, cell viability was determined by a methylene blue assay. ATP concentration was next expressed as %/NT/cell number.

ELISA. Conditioned media were collected after TRAIL treatment for indicated times and hTNF (DuoSet ELISA, R&D Systems Europe, Lille, France) was measured according to the manufacturer's instructions.

Western blot analysis. Immunoblotting analysis was performed as previously described.⁹ Revelation was performed by chemiluminescence using the LAS-3000 analyzer (Fujifilm, Bois-d'Arcy, France). Image processing and densitometry analyses were performed using Multi Gauge software (Fujifilm).

Cell transfections. HT29, HepG2, Jurkat, L929 and MEFs cells were transfected by reverse transfection with double-stranded siGenome SMARTpool siRNAs targeting mRNAs of hRIPK1 (ID = 8737), hRIPK3 (ID = 11 035), hFas/CD95 (ID = 355), hTNFR1 (ID = 7132), mTNFR1 (ID = 21 937), hPARP-1 (ID = 142), mPARP-1 (ID = 11 545) (ThermoFisher Scientific, Illkirch, France), or *Silencer Select* siRNA targeting mRNAs of hDR4 (ID = 8797) and hDR5 (ID = 8795) (Ambion, Applied Biosystems, Courtabouef, France). A non-specific targeting siRNA (siNT1, control siRNA, ThermoFisher Scientific) was used as a negative control for all experiments.

Cells were seeded in MW96 at a concentration of 20 000 cells/well for cell death assays and ATP measurement experiments. Per well, 80 nM siRNA and 0.3 μ l of DharmaFECT-4 transfection reagent (ThermoFisher Scientific) were applied in 25 μ l Opti-MEM1 (Invitrogen), for HT29, HepG2, L929 and MEFs cells. Then, 100 μ l cells/well was added. For Jurkat cells, 0.3 μ l of Lipofectamine LTX (Invitrogen) and 0.1 μ l of PLUS Reagent (Invitrogen) were used instead of DharmaFECT-4. Following a 72-h transfection period, cells were treated with TRAIL at pH 7.4 or 6.5, for indicated times.

Cells were seeded in MW6 at a concentration of 400 000 cells/well for immunoblotting experiments and PARP-1 activity measurements. Per well, 80 nM siRNA and 5 μ l of DharmaFECT-4 transfection reagent (ThermoFisher Scientific) were applied in 1 ml Opti-MEM1 (Invitrogen), for HT29, HepG2, L929 and MEFs cells. Then, 1 ml cells/well was added. For Jurkat cells, 5 μ l of Lipofectamine LTX (Invitrogen) and 2.5 μ l of PLUS Reagent (Invitrogen) were used instead of DharmaFECT-4. For immunoblotting, cells were harvested 72 h after transfection. For PARP-1 activity measurement, following a 72-h transfection period, cells were treated with TRAIL at pH 7.4 or 6.5, for 4 h.

RNA extraction and RT-qPCR analysis. Total RNA was extracted from cells using TRIzol reagent (Invitrogen) according to the manufacturer's instructions. To measure the relative mRNA levels of mTRAIL and mDR5, quantitative real-time RT-PCR was performed using Power SYBRGreen PCR (Applied Biosystems, Life Technologies), in conjunction with an ABI7300 real-time

PCR system (Applied Biosystems). Each sample was tested in duplicate in at least three independent experiments. rRNA 18S was used as the invariant control and primers efficiency was measured in each plate. The following primer sets were used. mTRAIL: 5'-CCCTGCTGCAGGTTAAGAG-3' (forward), 5'-GGCCTAAGGTCTTTCCATCC-3' (reverse); mDR5: 5'-TGACGGGGAAGAGGAAGTGA-3' (forward), 5'-GGCTTTGACCATTTGGATCT-3' (reverse).

PARP-1 activity assay. PARP-1 activity was measured with the PARP Universal Colorimetric Assay (Trevigen Inc., R&D Systems, Lille, France) according to the manufacturer's instructions. Briefly, 5×10^6 cells were lysed in PARP buffer containing 0.4 M NaCl, 1% Triton X-100 and proteases inhibitors; protein concentration was determined by Bradford assay and at least 20 μ g of protein were used in triplicate to measure, by a colorimetric assay, the incorporation of biotinylated PAR onto histone proteins coated in a 96-well plate. PARP-1 activity was expressed as arbitrary units.

Measurement of intracellular superoxide anion by flow cytometry. Dihydroethidium (DHE, Molecular Probes, Life Technologies) was used to detect intracellular superoxide anion ($O_2^{\cdot-}$) production. After treatment, floating and adherent cells (1×10^6 cells) were recovered, washed and incubated in PBS containing 5 μ M DHE for 30 min at 37°C. Dye oxidation (increase in FL-2 fluorescence) was measured using a FC-500 flow cytometer (Beckman Coulter). A positive control was obtained by incubating cells for 1 h with Menadione (100 μ M). Each measurement was conducted on 10 000 cells and analyzed on CXP Analysis (Beckman Coulter). Superimposition of control and Menadione histograms allowed defining a gate for calculating the percentage of cells with accumulated superoxide anion.

Con A-induced hepatitis. Seven to nine-week-old female C57Bl/6 WT (Janvier, Le Genest St. Isle, France) or CD1d KO mice (provided by Dr. A Leluen, Hôpital St. Vincent de Paul, INSERM U986, Paris) were treated with a retro-orbital administration of 20 mg/kg Con A (Sigma-Aldrich) diluted in PBS. Mice were killed at 6 h (WT, $n=6$; CD1d KO, $n=7$) or 10 h (WT, $n=7$; CD1d KO, $n=6$) following treatment. Control mice were treated with vehicle only (PBS) (WT, $n=7$; CD1d KO, $n=6$). All mice used were bred in our local house facilities.

For Nec-1 and PJ-34 experiment, C57Bl/6 WT mice were pretreated with i.p. administration of 10 mg/kg PJ-34 for 1 h, or i.v. administration of 125 μ g Nec-1 for 15 min, or with both inhibitors before i.v. administration of 12 mg/kg Con A for 10 h. At the end of treatment, mice were killed (PBS + Con A, $n=10$; Nec-1 + Con A, $n=6$; PJ-34 + Con A, $n=6$; PJ-34 + Nec-1 + Con A, $n=7$). Control mice were treated with Nec-1 + PBS ($n=7$), PJ-34 + PBS ($n=7$) or PJ-34 + Nec-1 + PBS ($n=7$). All animals received human care and all study protocols comply with the institution's guidelines.

Fragments of mouse livers were fixed in 4% paraformaldehyde and embedded in paraffin for Hematoxylin/Eosin staining. Serum AST and ALT were measured in serum according to the IFCC primary reference procedures and using the Olympus AU2700 Autoanalyser (Olympus France, Rungis, France).

For liver lysates preparation, 100 mg of liver was homogenized on ice in 650 μ l PARP assay lysis buffer containing 0.4 M NaCl, 1% Triton X-100 and proteases inhibitors, with an ULTRA-TURRAX homogenizer. Lysates were incubated on ice with periodic vortexing for 40 min, and then centrifuged at 10 000 $\times g$ for 10 min at 4°C to remove insoluble material. Protein concentration was determined by Bradford assay before further analysis.

Statistical analyses. Data presented were acquired from a minimum of three independent experiments. They are expressed as means \pm S.D. Statistical analyses for *in vitro* studies were performed with a Student's *t*-test considering the variances as unequal. For *in vivo* studies, Mann-Whitney *U* test was used for comparison of control group parameters with treatment group and multiple group analysis was carried out by one-way ANOVA with post Mann-Whitney *U* test. The correlation between continuous variables was examined using Spearman's rank-order coefficients. All statistical analyses were performed with GraphPad Prism5 software (GraphPad Software, San Diego, CA, USA). The significance is shown as follows: * $P < 0.05$, ** $P < 0.01$ and *** $P < 0.001$, TRAIL versus NT. # $P < 0.05$, ## $P < 0.01$, ### $P < 0.001$, TRAIL with inhibitors versus TRAIL with DMSO, or TRAIL with specific siRNAs versus TRAIL with siNT1. $^{\S}P < 0.05$, $^{\S\S}P < 0.01$ and $^{\S\S\S}P < 0.001$, MEF KO cells versus MEF WT cells, or TRAIL pH 6.5 versus TRAIL pH 7.4. And for the *in vivo* experiments: * $P < 0.05$, ** $P < 0.01$ and *** $P < 0.001$, mice treated with Con A versus mice treated with PBS.

[#]*P* < 0.05, ^{##}*P* < 0.01 and ^{###}*P* < 0.001, CD1d KO mice treated with Con A versus WT mice treated with Con A. [§]*P* < 0.05, ^{§§§}*P* < 0.001, mice treated with Nec-1 + ConA, PJ-34 + Con A or Nec-1 + PJ-34 + Con A versus mice treated with PBS + Con A.

Conflict of Interest

The authors declare no conflict of interest.

Acknowledgements. We are grateful to Dr. Alicia Torriglia and Dr. Mathieu Bertrand for helpful discussions. We thank in particular Linde Duprez and Mathieu Bertrand for preparing and making available *ripk1* and *ripk3* knockout MEF cells. We also thank the animal house facilities, the flow cytometry platform and the immunohistology platform (SFR Biosit, Rennes). Research in the IRSET group was supported by grants from the Ligue Nationale Contre le Cancer (the Côte d'Armor, Ille et Vilaine, Morbihan, Vendée and Sarthe Committees), INSERM, University of Rennes 1 and the Region Bretagne. S Jouan-Lanhouet was supported by the Association pour la Recherche sur le Cancer (doctoral fellowship). Research in the Vandenaabeele group has been supported by Flanders Institute for Biotechnology (VIB), by European grants (FP6 ApopTrain, MRTN-CT-035624; FP7 EC RTD Integrated Project, Apo-Sys, FP7-200767; Euregional PACT II), Belgian grants (Interuniversity Attraction Poles, IAP 6/18), Flemish grants (Fonds Wetenschappelijk Onderzoek Vlaanderen, FWO G.0875.11 and FWO G.0973.11) and Ghent University grants (MRP, GROUP-ID). P Vandenaabeele is also holder of a Methusalem grant (BOF09/01M00709) from the Flemish Government.

- Ashkenazi A, Pai RC, Fong S, Leung S, Lawrence DA, Marsters SA *et al*. Safety and antitumor activity of recombinant soluble Apo2 ligand. *J Clin Invest* 1999; **104**: 155–162.
- Takeda K, Hayakawa Y, Smyth MJ, Kayagaki N, Yamaguchi N, Kakuta S *et al*. Involvement of tumor necrosis factor-related apoptosis-inducing ligand in surveillance of tumor metastasis by liver natural killer cells. *Nat Med* 2001; **7**: 94–100.
- Zheng SJ, Wang P, Tsabary G, Chen YH. Critical roles of TRAIL in hepatic cell death and hepatic inflammation. *J Clin Invest* 2004; **113**: 58–64.
- Gonzalvez F, Ashkenazi A. New insights into apoptosis signaling by Apo2L/TRAIL. *Oncogene* 2010; **29**: 4752–4765.
- Wu GS, Burns TF, Zhan Y, Alnemri ES, El-Deiry WS. Molecular cloning and functional analysis of the mouse homologue of the KILLER/DR5 tumor necrosis factor-related apoptosis-inducing ligand (TRAIL) death receptor. *Cancer Res* 1999; **59**: 2770–2775.
- Holler N, Zaru R, Micheau O, Thome M, Attinger A, Valitutti S *et al*. Fas triggers an alternative, caspase-8-independent cell death pathway using the kinase RIP as effector molecule. *Nat Immunol* 2000; **1**: 489–495.
- Kemp TJ, Kim JS, Crist SA, Griffith TS. Induction of necrotic tumor cell death by TRAIL/Apo-2L. *Apoptosis* 2003; **8**: 587–599.
- Meurette O, Huc L, Rebillard A, Le Moigne G, Lagadic-Gossmann D, Dimanche-Boitrel MT. TRAIL (TNF-related apoptosis-inducing ligand) induces necrosis-like cell death in tumor cells at acidic extracellular pH. *Ann NY Acad Sci* 2005; **1056**: 379–387.
- Meurette O, Rebillard A, Huc L, Le Moigne G, Merino D, Micheau O *et al*. TRAIL induces receptor-interacting protein 1-dependent and caspase-dependent necrosis-like cell death under acidic extracellular conditions. *Cancer Res* 2007; **67**: 218–226.
- Lardner A. The effects of extracellular pH on immune function. *J Leukoc Biol* 2001; **69**: 522–530.
- Wike-Hooley JL, van den Berg AP, van der Zee J, Reinhold HS. Human tumour pH and its variation. *Eur J Cancer Clin Oncol* 1985; **21**: 785–791.
- Boujrad H, Gubkina O, Robert N, Krantic S, Susin SA. AIF-mediated programmed necrosis: a highly regulated way to die. *Cell Cycle* 2007; **6**: 2612–2619.
- Degterev A, Huang Z, Boyce M, Li Y, Jagtap P, Mizushima N *et al*. Chemical inhibitor of nonapoptotic cell death with therapeutic potential for ischemic brain injury. *Nat Chem Biol* 2005; **1**: 112–119.
- Vandenaabeele P, Galluzzi L, Vanden Berghe T, Kroemer G. Molecular mechanisms of necroptosis: an ordered cellular explosion. *Nat Rev Mol Cell Biol* 2010; **11**: 700–714.
- Andrabi SA, Dawson TM, Dawson VL. Mitochondrial and nuclear cross talk in cell death: parthanatos. *Ann NY Acad Sci* 2008; **1147**: 233–241.
- Degterev A, Yuan J. Expansion and evolution of cell death programmes. *Nat Rev Mol Cell Biol* 2008; **9**: 378–390.
- Cho YS, Challa S, Moquin D, Genga R, Ray TD, Guildford M *et al*. Phosphorylation-driven assembly of the RIP1-RIP3 complex regulates programmed necrosis and virus-induced inflammation. *Cell* 2009; **137**: 1112–1123.
- He S, Wang L, Miao L, Wang T, Du F, Zhao L *et al*. Receptor interacting protein kinase-3 determines cellular necrotic response to TNF- α . *Cell* 2009; **137**: 1100–1111.
- Zhang DW, Shao J, Lin J, Zhang N, Lu BJ, Lin SC *et al*. RIP3, an energy metabolism regulator that switches TNF-induced cell death from apoptosis to necrosis. *Science* 2009; **325**: 332–336.
- Tiegs G, Gantner F. Immunotoxicology of T cell-dependent experimental liver injury. *Exp Toxicol Pathol* 1996; **48**: 471–476.
- Kaneko Y, Harada M, Kawano T, Yamashita M, Shibata Y, Gejyo F *et al*. Augmentation of α Galactose 14 NKT cell-mediated cytotoxicity by interleukin 4 in an autocrine mechanism resulting in the development of concanavalin A-induced hepatitis. *J Exp Med* 2000; **191**: 105–114.
- Takeda K, Hayakawa Y, Van Kaer L, Matsuda H, Yagita H, Okumura K. Critical contribution of liver natural killer T cells to a murine model of hepatitis. *Proc Natl Acad Sci USA* 2000; **97**: 5498–5503.
- Toyabe S, Seki S, Iiai T, Takeda K, Shirai K, Watanabe H *et al*. Requirement of IL-4 and liver NK1 + T cells for concanavalin A-induced hepatic injury in mice. *J Immunol* 1997; **159**: 1537–1542.
- Schulze-Osthoff K, Bakker AC, Vanhaesebroeck B, Beyaert R, Jacob WA, Fiers W. Cytotoxic activity of tumor necrosis factor is mediated by early damage of mitochondrial functions. Evidence for the involvement of mitochondrial radical generation. *J Biol Chem* 1992; **267**: 5317–5323.
- Goossens V, De Vos K, Vercaemmen D, Steemans M, Vancompernelle K, Fiers W *et al*. Redox regulation of TNF signaling. *Biofactors* 1999; **10**: 145–156.
- Jan G, Belzacq AS, Haouzi D, Rouault A, M \acute{e} tivier D, Kroemer G *et al*. Propionibacteria induce apoptosis of colorectal carcinoma cells via short-chain fatty acids acting on mitochondria. *Cell Death Differ* 2002; **9**: 179–188.
- Degterev A, Hitomi J, Germscheid M, Ch'en IL, Korkina O, Teng X *et al*. Identification of RIP1 kinase as a specific cellular target of necrostatins. *Nat Chem Biol* 2008; **4**: 313–321.
- Hitomi J, Christofferson DE, Ng A, Yao J, Degterev A, Xavier RJ *et al*. Identification of a molecular signaling network that regulates a cellular necrotic cell death pathway. *Cell* 2008; **135**: 1311–1323.
- Festjens N, Vanden Berghe T, Vandenaabeele P. Necrosis, a well-orchestrated form of cell demise: signalling cascades, important mediators and concomitant immune response. *Biochim Biophys Acta* 2006; **1757**: 1371–1387.
- Temkin V, Huang Q, Liu H, Osada H, Pope RM. Inhibition of ADP/ATP exchange in receptor-interacting protein-mediated necrosis. *Mol Cell Biol* 2006; **26**: 2215–2225.
- Los M, Mozoluk M, Ferrari D, Stepczynska A, Stroh C, Renz A *et al*. Activation and caspase-mediated inhibition of PARP: a molecular switch between fibroblast necrosis and apoptosis in death receptor signaling. *Mol Biol Cell* 2002; **13**: 978–988.
- Wang Y, Dawson VL, Dawson TM. Poly(ADP-ribose) signals to mitochondrial AIF: a key event in parthanatos. *Exp Neurol* 2009; **218**: 193–202.
- Vanden Berghe T, Kalai M, van Loo G, Declercq W, Vandenaabeele P. Disruption of HSP90 function reverts tumor necrosis factor-induced necrosis to apoptosis. *J Biol Chem* 2003; **278**: 5622–5629.
- Xu Y, Huang S, Liu ZG, Han J. Poly(ADP-ribose) polymerase-1 signaling to mitochondria in necrotic cell death requires RIP1/TRAF2-mediated JNK1 activation. *J Biol Chem* 2006; **281**: 8788–8795.
- Gagne JP, Moreel X, Gagne P, Labelle Y, Droit A, Chevalier-Paré M *et al*. Proteomic investigation of phosphorylation sites in poly(ADP-ribose) polymerase-1 and poly(ADP-ribose) glycohydrolase. *J Proteome Res* 2009; **8**: 1014–1029.
- Christofferson DE, Yuan J. Cyclophilin A release as a biomarker of necrotic cell death. *Cell Death Differ* 2010; **17**: 1942–1943.
- Scaffidi P, Misteli T, Bianchi ME. Release of chromatin protein HMGB1 by necrotic cells triggers inflammation. *Nature* 2002; **418**: 191–195.
- Sass G, Heinlein S, Agli A, Bang R, Sch \ddot{u} mann J, Tiegs G. Cytokine expression in three mouse models of experimental hepatitis. *Cytokine* 2002; **19**: 115–120.
- Hu X, Han W, Li L. Targeting the weak point of cancer by induction of necroptosis. *Autophagy* 2007; **3**: 490–492.
- Lepretre C, Scovassi AI, Shah GM, Torriglia A. Regulation of poly(ADP-ribose) polymerase-1 functions by leukocyte elastase inhibitor/LEI-derived DNase II during caspase-independent apoptosis. *Int J Biochem Cell Biol* 2009; **41**: 1046–1054.

Supplementary Information accompanies the paper on Cell Death and Differentiation website (<http://www.nature.com/cdd>)